electronic reprint

STRUCTURAL BIOLOGY
COMMUNICATIONS

ISSN: 2053-230X
journals.iucr.org/f

Phosphate-binding protein from *Polaromonas* JS666: purification, characterization, crystallization and sulfur SAD phasing

Vanessa R. Pegos, Louis Hey, Jacob LaMirande, Rachel Pfeffer, Rosalie Lipsh, Moshe Amitay, Daniel Gonzalez and Mikael Elias

Acta Cryst. (2017). F**73**, 342–346

STRUCTURAL BIOLOGY COMMUNICATIONS

ISSN 2053-230X

Phosphate-binding protein from *Polaromonas* JS666: purification, characterization, crystallization and sulfur SAD phasing

Vanessa R. Pegos,[a] Louis Hey,[a] Jacob LaMirande,[a] Rachel Pfeffer,[b] Rosalie Lipsh,[b] Moshe Amitay,[b] Daniel Gonzalez[c] and Mikael Elias[a]*

[a]Biochemistry, Molecular Biology and Biophysics Department and BioTechnology Institute, University of Minnesota, Saint Paul, MN 55108, USA, [b]Department of Bioinformatics, The Jerusalem College of Technology – Lev Academic Center, Jerusalem 91160, Israel, and [c]URMITE, Aix Marseille Université, INSERM, CNRS, IRD, 27 Boulevard Jean Moulin, 13385 Marseille, France. *Correspondence e-mail: mhelias@umn.edu

Received 24 February 2017
Accepted 19 May 2017

Edited by I. Tanaka, Hokkaido University, Japan

Keywords: phosphate-binding protein; phosphate ABC transporter; molecular specificity; *Polaromonas* JS666.

Phosphate-binding proteins (PBPs) are key proteins that belong to the bacterial ABC-type phosphate transporters. PBPs are periplasmic (or membrane-anchored) proteins that capture phosphate anions from the environment and release them to the transmembrane transporter. Recent work has suggested that PBPs have evolved for high affinity as well as high selectivity. In particular, a short, unique hydrogen bond between the phosphate anion and an aspartate residue has been shown to be critical for selectivity, yet is not strictly conserved in PBPs. Here, the PBP from *Polaromonas* JS666 is focused on. Interestingly, this PBP is predicted to harbor different phosphate-binding residues to currently known PBPs. Here, it is shown that the PBP from *Polaromonas* JS666 is capable of binding phosphate, with a maximal binding activity at pH 8. Its structure is expected to reveal its binding-cleft configuration as well as its phosphate-binding mode. Here, the expression, purification, characterization, crystallization and X-ray diffraction data collection to 1.35 Å resolution of the PBP from *Polaromonas* JS666 are reported.

1. Introduction

Phosphate is an essential resource for living organisms (Westheimer, 1987), yet it is very limiting, being mostly trapped in rocks (Cordell *et al.*, 2009). Therefore, microorganisms have evolved efficient systems to capture phosphate from their environments (Hsieh & Wanner, 2010). The predominant bacterial phosphate transporter Pst (Hsieh & Wanner, 2010) is an ABC transporter and is composed of five proteins: two membrane permeases (PstA and PstC), two ATPases (PstB) and the high-affinity phosphate-binding protein PstS (Lamarche *et al.*, 2008). It is a high-affinity, high-specificity transporter that enables microorganisms to extract phosphate (Hsieh & Wanner, 2010), including from environments in which competing anions are plentiful, such as arsenate-rich niches (Elias *et al.*, 2012).

The solute-binding protein (PstS), also known as phosphate-binding protein (PBP), is responsible for the capture of the anion and its release into the transporter channel. Crystal structures of a range of PBPs have previously been determined (Vyas *et al.*, 2003; Luecke & Quiocho, 1990; Brautigam *et al.*, 2014; Liebschner *et al.*, 2009). PBP structures are composed of two globular domains, consisting of a central β-sheet core flanked by an α-helix, linked together with a flexible hinge (Felder *et al.*, 1999). The bound phosphate anion lies at the interface of the domains, completely buried in a cleft. The anion is bound *via* a large number of hydrogen

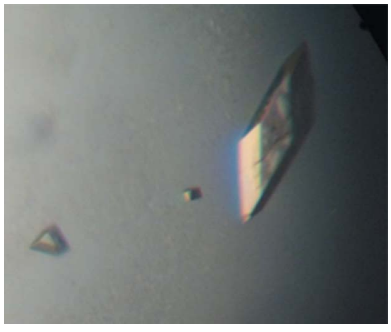

bonds: in most characterized PBPs it makes 12 hydrogen bonds to the protein [*e.g.* in PfluDING (Liebschner *et al.*, 2009; Moniot *et al.*, 2007; Ahn *et al.*, 2007) and in the PBPs from *Mycobacterium tuberculosis*, *Escherichia coli*, *Yersinia pestis* and *Stenotrophomonas maltophilia* (Luecke & Quiocho, 1990; Liebschner *et al.*, 2009; Tanabe *et al.*, 2007; Keegan *et al.*, 2016)]. In others, it is bound *via* a constellation of 14 hydrogen bonds (*e.g.* in *Clostridium perfringens* PBP-1; Gonzalez *et al.*, 2014). Most of the PBPs characterized to date possess a key aspartate residue that forms a putative low-barrier hydrogen bond (LBHB) to the bound anion (Elias *et al.*, 2012). This unique, short bond has previously been shown to be involved in the exquisite selectivity of the phosphate transporter, enabling it to prefer phosphate over arsenate by around three orders of magnitude (Elias *et al.*, 2012) and phosphate over sulfate by around five orders of magnitude (Elias *et al.*, 2012; Luecke & Quiocho, 1990). *C. perfringens* PBP-1, which does not make an LBHB with the bound phosphate anion, has recently been shown to exhibit reduced selectivity (Gonzalez *et al.*, 2014).

Here, we focus on the PBP from *Polaromonas* JS666 (Mattes *et al.*, 2008), a Gram-negative bacterium that is a psychrophile. *Polaromonas* species tend to live in marine environments, including the Antarctic Ocean. Interestingly, phosphate levels in oceanic waters are generally low (∼1 µ*M*; Kattner, 1999). *Polaromonas* JS666 has been identified in very diverse environments, such as groundwater contaminated by arsenate in West Bengal in India (Paul *et al.*, 2015). *Polaromonas* JS666 has also previously been investigated by virtue of its ability to biodegrade the toxic compound *cis*-1,2-dichloroethene (Giddings *et al.*, 2010).

Here, we report the expression and purification of the PBP from *Polaromonas* JS666 (WP_011482582.1). Although this protein is annotated as being associated with the bacterial Pst transporter, there is no evidence that this PBP is associated with an ABC transporter. We report its crystallization and preliminary X-ray diffraction analysis, as well as its pH preference for phosphate binding.

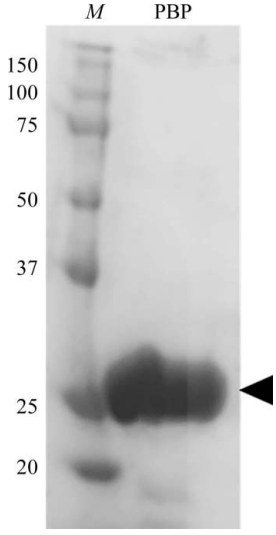

Figure 1
12%(*w*/*v*) SDS–PAGE of the PBP from *Polaromonas* JS666. Lane *M* contains molecular-weight markers (Precision Plus Protein Kaleidoscope Prestained Protein Standards, Bio-Rad). The second lane contains 5 µl PBP at 8.5 mg ml^{-1} (indicated by a black arrow). The molecular weights of the markers are indicated in kDa.

Table 1
Production of the PBP from *Polaromonas* JS666.

Source organism	*Polaromonas* JS666
DNA source	Synthetic
Cloning vector	pET-22b(+)
Expression vector	pET-22b(+)
Restriction sites	NdeI, NotI
Expression host	*E. coli* BL21(DE3)
Complete amino-acid sequence of the construct produced	MGIVLDGSSGMLPLAKALASAYQQRSSDPQVEIG- KGLGAGARLRALAEGKIQIALASHGITPEDVQ- KGNLKIIEVAKGAIVFAVNASVPITNFTESQV- CDAYSGKIRSWQPLGGSDNSVAVLTRPPTEVD- PEVIRAKVGCFKELKEIETAKVMARGGDMAKA- LAETPYALGMTSMTVVEQSAGKVRALTLNGIA- PTAENVKSGRYFLTRDFLFVIKGEPTGPVKRF- LDFVLSPEGDRAIQANGAVPLRAAALEHHHHHH

2. Materials and methods

2.1. Production of the PBP from *Polaromonas* JS666

The *pbp* gene (encoding the protein WP_011482582.1) was codon-optimized for heterologous expression in *E. coli* and synthesized by GenScript (Piscataway, New Jersey, USA; Table 1). The mature gene (without the signal peptide) was cloned in pET-22b(+) (Novagen) using NdeI and NotI restriction sites. Protein production and purification was performed in *E. coli* BL21(DE3) cells in LB medium supplemented with ampicillin (100 µg ml^{-1}). Cultures were grown at 37°C to an $OD_{600\,nm}$ of 0.6 and were then induced with 1 m*M* IPTG and a temperature transition to 18°C over 15 h.

The cells were harvested by centrifugation (4000*g* at 4°C for 15 min) and the pellets were frozen at −20°C before purification. The pellets were resuspended in lysis buffer (50 m*M* Tris–HCl, 100 m*M* NaCl pH 8.0, 0.1 m*M* PMSF) and the cells were disrupted by sonication (amplitude 35 for 45 s with 5 s pulses) on a QSonica device (Newtown, Connecticut, USA). The debris was removed by centrifugation (20 000*g* at 4°C for 45 min). The supernatant was loaded onto a nickel-affinity chromatography column (HisTrap HP, 5 ml; GE Healthcare) at a flow rate of 10 ml min^{-1}. Elution was performed using a buffer consisting of 50 m*M* Tris–HCl, 100 m*M* NaCl pH 8.0, 150 m*M* imidazole. A size-exclusion chromatography step (HiLoad 16/60, Superdex 200; GE Healthcare) was subsequently performed using a buffer consisting of 25 m*M* Tris–HCl pH 8.0, 100 m*M* NaCl. Protein production and purity were checked by 12%(*w*/*v*) SDS–PAGE (Fig. 1). The protein was concentrated to 7 mg ml^{-1} using a centrifugation device (Amicon Ultra MWCO 10 kDa; Millipore, Ireland) prior to crystallization trials. The protein was stored at 4°C. The production yield was approximately 2 mg per litre of culture.

2.2. Phosphate-binding assay

Phosphate-binding assays were performed to verify the ability of the *Polaromonas* PBP to bind phosphate and to

Table 2
Crystallization of the PBP from *Polaromonas* JS666.

Method	Vapor diffusion, hanging drop
Plate type	24-well plate
Temperature (K)	292
Protein concentration (mg ml^{-1})	7
Buffer composition of protein solution	50 m*M* Tris–HCl, 100 m*M* NaCl pH 8.0
Composition of reservoir solution	140 m*M* potassium bromide, 25% PEG 2000
Volume and ratio of drop	2 µl (1:1)
Volume of reservoir (µl)	500

determine the optimal pH (Fig. 2). In each assay, protein at 35 µ*M* was incubated with 1 n*M* 10 µCi [^{32}P]-phosphate for 86 h at 20°C with a final volume of 50 µl. The buffers used were composed of (i) 25 m*M* sodium acetate pH 4.5, 100 m*M* NaCl, (ii) 25 m*M* sodium citrate pH 6.0, 100 m*M* NaCl, (iii) 25 m*M* Tris–HCl pH 7.0, 100 m*M* NaCl, (iv) 25 m*M* Tris–HCl pH 7.5, 100 m*M* NaCl, (v) 25 m*M* Tris–HCl pH 8.0, 100 m*M* NaCl, (vi) 25 m*M* Tris–HCl pH 8.5, 100 m*M* NaCl, (vii) 25 m*M* CHES pH 9.0, 100 m*M* NaCl and (viii) 25 m*M* CHES pH 9.5, 100 m*M* NaCl. In order to read the samples, 25 µl of the assayed protein was immobilized on nitrocellulose membrane (Bio-Rad Nitrocellulose 0.45 µm) on a vacuum system (EMD Millipore XX2702550) and was extensively washed with 4 ml 10 m*M* Tris–HCl pH 8.0. The membrane was placed into scintillation tubes containing 4 ml scintillation solution (CytoScint-ES, MP Biomedicals) and the radioactivity was read using a scintillation counter (Beckman Coulter LS6000). Experiments were conducted in triplicate. As a control, the same procedure was used with 65 µ*M* bovine serum albumin (Akron Biotech).

2.3. Crystallization

Concentrated samples of PBP (7 mg ml^{-1}) were submitted to crystallization trials at the University of Minnesota Nanoliter Crystallization Facility. Assays were performed using the sitting-drop vapor-diffusion method set up in a 96-well plate using the JCSG+ commercial screening kit. The tested ratios were 1:1, 1:2 and 1:3 precipitant:protein (Table 2). The plates were incubated at 292 K. The best condition consisted of 140 m*M* potassium bromide, 25%(*w*/*v*) PEG 2000 with a 1:1 precipitant:protein ratio. The initial crystals yielded poor, highly mosaic diffraction patterns. Fresh crystals (∼5) were transferred into a microtube containing 50 µl mother liquor and were mechanically broken. The seed solution was diluted 100-fold. Fresh microseeding was performed by adding 0.1 µl seed solution to the 2 µl drops and yielded better crystals. Diffraction-quality crystals appeared after 20 d at 292 K (Fig. 3).

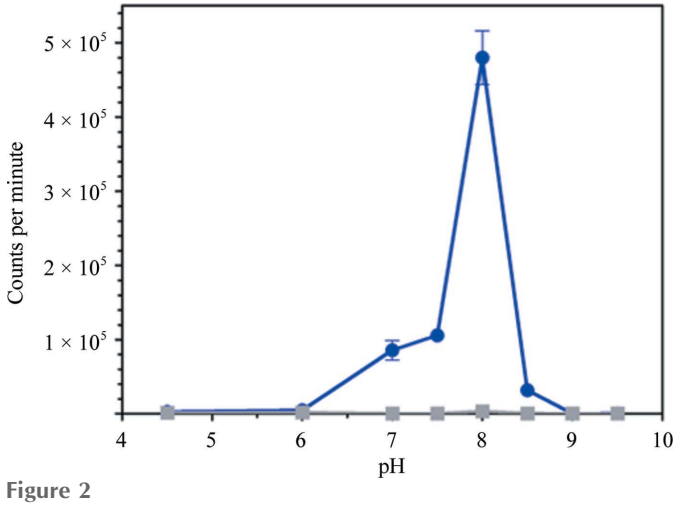

Figure 2
Phosphate-binding ability and its pH dependence. The phosphate-binding activity of radiolabeled phosphate (in counts per minute) for the PBP (in blue) and for bovine serum albumin (in gray) is shown at varying pH values.

Table 3
Data collection and processing.

Values in parentheses are for the outer shell.

	S-SAD merged set	High-resolution data set
Diffraction source	Home source	23-ID-B, APS
Wavelength (Å)	2.2909	1.0332
Temperature (K)	100	100
Detector	R-AXIS IV^{++} image plate	PILATUS 6M
Crystal-to-detector distance (mm)	150.7	150.0
Rotation range per image (°)	0.5	1
Total rotation range (°)	793.5	250
Exposure time per image (s)	40	0.2
Space group	*C*2	*C*2
a, *b*, *c* (Å)	117.79, 38.38, 58.26	117.52, 38.48, 58.34
α, *β*, *γ* (°)	90.0, 114.7, 90.0	90.0, 114.0, 90.0
Resolution (Å)	2.48 (2.60–2.48)	1.35 (1.45–1.35)
Total No. of reflections	122201 (11653)	257565 (49660)
No. of unique reflections	16370 (2108)	51937 (9883)
Completeness (%)	99.2 (96.9)	98.5 (97.9)
Multiplicity	7.46 (5.52)	4.95 (5.02)
$\langle I/\sigma(I)\rangle$	47.33 (18.30)	58.56 (7.89)
$R_{\rm r.i.m.}$ (%)	6.7 (10.1)	3.3 (19.8)

2.4. Data collection and processing

Crystals were mounted on a CryoLoop (Hampton Research) and flash-cooled at 100 K in liquid nitrogen using the mother liquor as cryoprotectant. The first set of diffraction

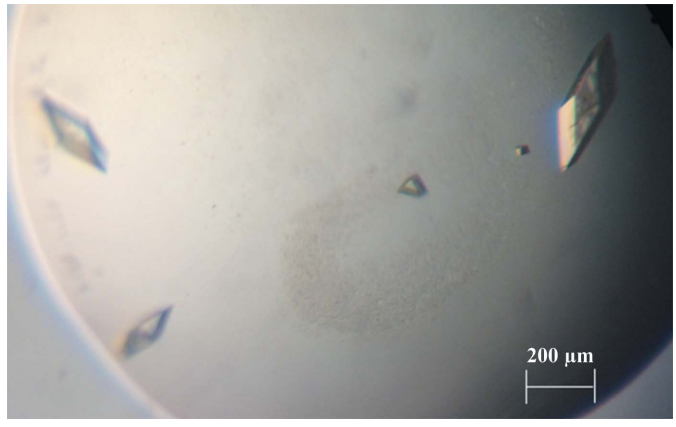

Figure 3
Crystals of the PBP from *Polaromonas* JS666 after microseeding

data was collected on the home source (Rigaku–MSC MicroMax-007 X-ray generator) using a chromium anode. Data collection was performed using an R-AXIS IV^{++} image-plate detector, a wavelength of 2.2909 Å and 40 s exposures. Individual frames consisted of 0.5° steps. A total of four different data sets were collected from four different crystals to give a total of 1587 images. The data sets were indexed, integrated, scaled and merged using the *XDS* package (Kabsch, 1993). The merged data set is complete (99.2%) and has a redundancy of 7.46 at 2.48 Å resolution. A second data set was collected on beamline 23-ID-D at the Advanced Photon Source (APS), Argonne, Illinois, USA to a higher resolution (1.35 Å) using a wavelength of 1.03 Å, a PILATUS 6M detector, 0.2 s exposure time and 0.5° oscillation (Table 3, Fig. 4). This data set was indexed, integrated and scaled using the *XDS* package (Kabsch, 1993). We note that the high intensities at high resolution indicate that higher resolution data may be collected in the future.

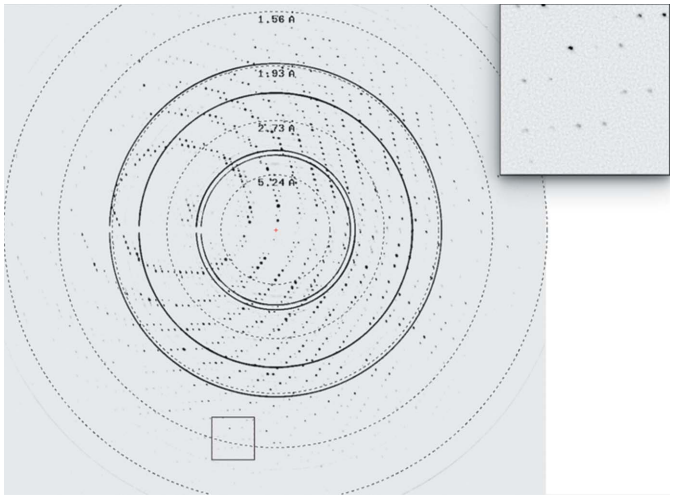

Figure 4
A diffraction frame from a crystal of PBP. The rectangle in the diffraction frame indicates the location of the enlarged portion at the top right. The edge of the frame is at 1.35 Å resolution.

3. Results and discussion

In this study, we demonstrate that the PBP from *Polaromonas* JS666 is a phosphate-binding protein that shows maximum phosphate-binding activity at pH 8 and shows no binding at low pH. Similar observations were made with other PBPs: the PBP from *E. coli* was reported to bind phosphate with lower affinity at pH 4.5 (Wang *et al.*, 1997), and no binding was observed at pH 4.5 for human PBP (Morales *et al.*, 2006). These observations were subsequently related to the observed preference of PBPs for the dibasic form of phosphate in sub-Ångstrom crystallization studies (Liebschner *et al.*, 2009; Elias *et al.*, 2012). Intriguingly, the binding residues of phosphate-binding proteins are not strictly conserved (Vyas *et al.*, 2003; Gonzalez *et al.*, 2014). Major residues have been shown to change, including the aspartate residue involved in the key, discriminating, short hydrogen bond to the anion as observed in PfluDING (Liebschner *et al.*, 2009; Moniot *et al.*, 2007; Ahn *et al.*, 2007) and the *E. coli* PBP (Luecke & Quiocho, 1990), which is replaced by a serine residue in *C. perfringens* PBP-1 (Gonzalez *et al.*, 2014). A deeper analysis of the phosphate-binding family, which will be published elsewhere, allowed us to isolate PBPs with very different predicted phosphate-binding pockets, including the PBP from *Polaromonas* JS666. A sequence alignment of various PBPs (Fig. 5) reveals that the PBP from *Polaromonas* JS666 is predicted to harbor residues in its phosphate-binding cleft that are significantly different

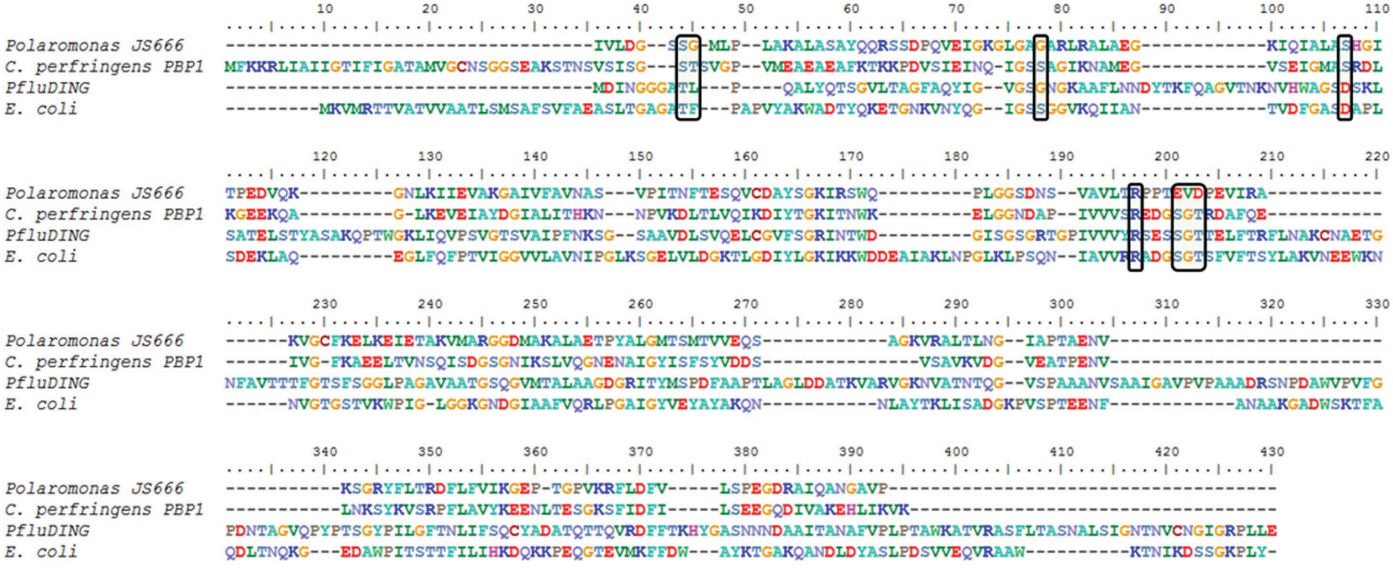

Figure 5
Alignment of phosphate-binding proteins, including the PBPs from *Polaromonas* JS666, *E. coli*, *Pseudomonas fluorescens* (PfluDING) and *Clostridium perfringens* (PBP1), performed with the *MUSCLE* program with default parameters (Edgar, 2004). The black boxes highlight the residues that are involved in phosphate binding in *C. perfringens* PBP1, *E. coli* PBP and PfluDING, and the residues that are predicted to bind phosphate in the *Polaromonas* JS666 PBP.

(with four out of eight differing) from all currently known PBPs. Whereas this observation may be surprising, it is important to note that most of the PBP–anion bonds typically involve main-chain NH groups (seven out of the 12 interactions observed in PfluDING involve the main chain). These main-chain interactions might explain why some of these residues can be substituted. With this new structure, we expect to unravel a new phosphate-binding mode that is predicted to involve two negatively charged residues: a glutamate and an aspartate. The understanding of this binding mode, and the determination of the binding properties of this protein, may provide insights into how *Polaromonas* JS666 captures phosphate, including in phosphate-depleted environments such as oceanic waters.

We have therefore produced, crystallized and collected data sets for *Polaromonas* JS666 PBP. The crystals belonged to space group *C*2, with unit-cell parameters $a = 117.52$, $b = 38.48$, $c = 58.34$ Å, $\alpha = \gamma = 90$, $\beta = 114.0^\circ$. The PBP has a molecular weight of 29 kDa, and a Matthews coefficient calculation suggests the presence of one monomer in the asymmetric unit with 40% solvent content. Initial molecular replacements were attempted using the closest known structure (PBP-1 from *C. perfringens*; PDB entry 4q8r; Gonzalez *et al.*, 2014; 31% identity) in *Phaser* (McCoy *et al.*, 2007) and *MOLREP* (Vagin & Teplyakov, 2010), and were unsuccessful.

We collected four data sets using four different crystals at a wavelength of 2.2909 Å that were subsequently merged into a single data set that was used for phasing and is presented in Table 3. The *Polaromonas* JS666 sequence contains six methionine residues and two cysteine residues. Experimental phasing was performed using *PHENIX* (Adams *et al.*, 2010). An anomalous signal analysis performed with *phenix.xtriage* (Adams *et al.*, 2010) indicates that the measurability of the anomalous signal extends to 2.5 Å resolution. During the substructure search, nine sites were found (with occupancies of 1.51, 1.24, 1.24, 1.05, 0.71, 0.85, 0.75, 0.81 and 0.64), which also include the P atom from the bound phosphate. The *AutoSol* program in *PHENIX* proposed the best solution with a figure of merit of 0.448 and a Bayesian correlation coefficient of 43.68 ± 9.88. After density modification, the *R* factor, the map skew factor and the correlation of local r.m.s. density were 27.42%, 0.17 and 0.78, respectively. Automated model building constructed 212 residues (out of a total of 247) in 14 fragments, and placed 62 water molecules, with an $R_{\rm free}$ and $R_{\rm work}$ of 0.37 and 0.30, respectively. Manual model building was performed using *Coot* (Emsley *et al.*, 2010) and refinement against the 1.35 Å resolution data was performed using *REFMAC* (Murshudov *et al.*, 2011). Structure refinement is in progress (after nine cycles of refinement, $R_{\rm free}$ and $R_{\rm work}$ were 0.22 and 0.17, respectively). Structure resolution and interpretation are also currently in progress.

Acknowledgements

We are grateful to the Nano Crystallization Facility and the Kahlert Structural Biology Laboratory, and in particular to Carrie Wilmot and Ke Shi for assistance in setting up crystallization screens and to Ed Hoeffner for assistance in using the in-house X-ray diffraction setup.

Funding information

Funding for this research was provided by: MnDrive Initiative; University of Minnesota Grand Challenges program.

References

Adams, P. D. *et al.* (2010). *Acta Cryst.* D**66**, 213–221.
Ahn, S., Moniot, S., Elias, M., Chabriere, E., Kim, D. & Scott, K. (2007). *FEBS Lett.* **581**, 3455–3460.
Brautigam, C. A., Ouyang, Z., Deka, R. K. & Norgard, M. V. (2014). *Protein Sci.* **23**, 200–212.
Cordell, D., Drangert, J.-O. & White, S. (2009). *Glob. Environ. Change*, **19**, 292–305.
Edgar, R. C. (2004). *Nucleic Acids Res.* **32**, 1792–1797.
Elias, M., Wellner, A., Goldin-Azulay, K., Chabriere, E., Vorholt, J. A., Erb, T. J. & Tawfik, D. S. (2012). *Nature (London)*, **491**, 134–137.
Emsley, P., Lohkamp, B., Scott, W. G. & Cowtan, K. (2010). *Acta Cryst.* D**66**, 486–501.
Felder, C. B., Graul, R. C., Lee, A. Y., Merkle, H.-P. & Sadee, W. (1999). *AAPS PharmSci*, **1**, E2.
Giddings, C. G., Liu, F. & Gossett, J. M. (2010). *Ground Water Monit. Remidiat.* **30**, 106–113.
Gonzalez, D., Richez, M., Bergonzi, C., Chabriere, E. & Elias, M. (2014). *Sci. Rep.* **4**, 6636.
Hsieh, Y.-J. & Wanner, B. L. (2010). *Curr. Opin. Microbiol.* **13**, 198–203.
Kabsch, W. (1993). *J. Appl. Cryst.* **26**, 795–800.
Kattner, G. (1999). *Mar. Chem.* **67**, 61–66.
Keegan, R., Waterman, D. G., Hopper, D. J., Coates, L., Taylor, G., Guo, J., Coker, A. R., Erskine, P. T., Wood, S. P. & Cooper, J. B. (2016). *Acta Cryst.* D**72**, 933–943.
Lamarche, M. G., Wanner, B. L., Crépin, S. & Harel, J. (2008). *FEMS Microbiol. Rev.* **32**, 461–473.
Liebschner, D., Elias, M., Moniot, S., Fournier, B., Scott, K., Jelsch, C., Guillot, B., Lecomte, C. & Chabrière, E. (2009). *J. Am. Chem. Soc.* **131**, 7879–7886.
Luecke, H. & Quiocho, F. A. (1990). *Nature (London)*, **347**, 402–406.
Mattes, T. E., Alexander, A. K., Richardson, P. M., Munk, A. C., Han, C. S., Stothard, P. & Coleman, N. V. (2008). *Appl. Environ. Microbiol.* **74**, 6405–6416.
McCoy, A. J., Grosse-Kunstleve, R. W., Adams, P. D., Winn, M. D., Storoni, L. C. & Read, R. J. (2007). *J. Appl. Cryst.* **40**, 658–674.
Moniot, S., Elias, M., Kim, D., Scott, K. & Chabriere, E. (2007). *Acta Cryst.* F**63**, 590–592.
Morales, R. *et al.* (2006). *Structure*, **14**, 601–609.
Murshudov, G. N., Skubák, P., Lebedev, A. A., Pannu, N. S., Steiner, R. A., Nicholls, R. A., Winn, M. D., Long, F. & Vagin, A. A. (2011). *Acta Cryst.* D**67**, 355–367.
Paul, D., Kazy, S. K., Gupta, A. K., Pal, T. & Sar, P. (2015). *PLoS One*, **10**, e0118735.
Tanabe, M., Mirza, O., Bertrand, T., Atkins, H. S., Titball, R. W., Iwata, S., Brown, K. A. & Byrne, B. (2007). *Acta Cryst.* D**63**, 1185–1193.
Vagin, A. & Teplyakov, A. (2010). *Acta Cryst.* D**66**, 22–25.
Vyas, N. K., Vyas, M. N. & Quiocho, F. A. (2003). *Structure*, **11**, 765–774.
Wang, Z., Luecke, H., Yao, N. & Quiocho, F. A. (1997). *Nature Struct. Biol.* **4**, 519–522.
Westheimer, F. H. (1987). *Science*, **235**, 1173–1178.